

1 **OM, SEM-EDX, Micro-Raman and FT-IR investigation of Roman frescoes from**
2 **Villa dei Quintili (Rome, Italy)**

3
4 Vincenza Crupi,^a Barbara Fazio,^b Giacomo Fiocco,^c Giuliana Galli,^d Mauro Francesco La Russa,^e
5 Maurizio Licchelli,^f Domenico Majolino,^a Marco Malagodi,^{*c,g} Michela Ricca,^e Silvestro Antonio
6 Ruffolo,^e Valentina Venuti^{§a}

7
8 ^a*Dipartimento di Scienze Matematiche e Informatiche, Scienze Fisiche e Scienze della Terra, Università degli Studi di*
9 *Messina, Viale Ferdinando Stagno D'Alcontres 31, 98166 Messina, Italy.*

10 ^b*CNR-IPCF Istituto per i Processi Chimico Fisici, viale F. Stagno d'Alcontres 37, Faro Superiore, I-98158 Messina,*
11 *Italy.*

12 ^c*Laboratorio Arvedi di Diagnostica non Invasiva, CISRiC, University of Pavia, Via Bell'Aspa 3, 26100 Cremona, Italy.*

13 ^d*Soprintendenza Speciale per i Beni Archeologici di Roma, Villa dei Quintili, via Appia Nuova 1092, 00197 Roma,*
14 *Italy.*

15 ^e*Dipartimento di Biologia, Ecologia e Scienze della Terra (DiBEST), Università degli Studi della Calabria, Via Pietro*
16 *Bucci, 87036 Arcavacata di Rende (Cs), Italy.*

17 ^f*Dipartimento di Chimica, Università di Pavia, Via Taramelli12, 27100 Pavia, Italy.* ^g*Dipartimento di*
18 *Musicologia e Beni Culturali, Università di Pavia, corso Garibaldi 178, 26100 Cremona, Italy.*

19
20 ^{*}Corresponding author. E-mail: marco.malagodi@unipv.it; Tel.: +390372567770.

21 [§]Corresponding author. E-mail: vvenuti@unime.it; Tel: +390906765299.

22
23
24 **Abstract**

25
26 The present work reports a multi-analytical study, based on optical microscopy (OM), scanning
27 electron microscopy equipped with an energy dispersive X-ray detector (SEM-EDX), micro-Raman
28 and Fourier transform infrared spectroscopy (FT-IR) techniques, aimed at establishing the painting
29 techniques and palettes used to decorate a variety of fragments of frescoes coming from Villa dei
30 Quintili in Rome (Italy) and dated back II century A. D.. This combined methodological approach,
31 covering different spatial scales extending from the macroscopic to the elemental domain, revealed
32 successful for the unambiguous identification, in non-invasive or at least micro-destructive way, of
33 pigments and binders. The used chromatic palette was identified as yellow ochre (goethite), carbon
34 black (of vegetal origin), green earth, red ochre (haematite), lime white and Egyptian blue
35 (cuprorivaite). Organic and inorganic binders were respectively identified as linseed oil and calcium
36 carbonate. Plaster layer was mainly composed by calcite, feldspars and gypsum.

37 The obtained data revealed crucial for improving our knowledge of materials and preparation methods
38 of pigmenting agents of these fragments, taken from the warehouse of the Villa and hence of
39 unknown provenance area, in view of their right positioning in a specific area of the archaeological
40 complex. In fact, the characterization of the different pigments could support the conservators to
41 better identify the distribution of the frescos among the different rooms and to reconstruct the original
42 aesthetic of the Villa during the Quintili age.

43
44

45 *Keywords:* micro-Raman spectroscopy; FT-IR spectroscopy; SEM-EDX; OM; Roman decorated
46 plasters; pigments.

47

48

49 **1. Introduction**

50

51 Since long time, the investigation of Roman wall paintings has attracted the interest of researchers
52 for many reasons. Frescos are, in fact, extended in a wide geographic area, in different architectural
53 contexts, exhibiting a variety of vivid colours. At present, even if many studies have been performed
54 from the artistic and archaeological points of view, we are still far from a comprehensive evaluation
55 of the employed materials and techniques (Bakiler et al., 2016; Mazzocchin et al., 2003).

56 In this context, the identification of pigments as well as of the composition of the plaster layers
57 used on the mural paintings represents one of the most important issue. As well known, it constitutes
58 the starting point for the understanding of the particular technique used from Roman artists in a
59 specific area (Barilaro et al., 2008). From that, the reconstruction of the possible communication and
60 trade routes can be, in principle, attempted.

61 An archaeometric investigation has been conducted on Roman plasters at different archaeological
62 sites, mainly in Italy, but not only (Aliatis et al., 2010; Amadori et al., 2015; Baraldi et al., 2007;
63 Duran et al., 2011; Edwards et al., 2003; Mahmoud et al., 2012; Mateos et al., 2015; Weber et al.,
64 2009). In all these cases, a multi-technique approach, involving both non-invasive and micro-
65 destructive methods such as Raman micro-spectroscopy, Fourier transform infrared spectroscopy
66 (FT-IR), scanning electron microscopy equipped with an energy dispersive X-ray detector (SEM-
67 EDX) and optical microscopy (OM), revealed successful in the determination of the plaster
68 composition and the nature of pigments.

69 Hence, an investigation has been carried out on some ancient Roman frescoes coming from Villa
70 dei Quintili (Rome, Italy) (Alberti et al., 2017; Crupi et al., 2015, 2016), in the framework of a wide

71 multi-technique archaeometric research performed on a variety of materials from this renowned
72 archaeological site (Belfiore et al., 2015).

73 Villa dei Quintili (Fig. 1) is a monumental complex located on the fifth mile of the via Appia
74 Antica, several kilometres far from the the center of Rome (Frontoni, 2000; Frontoni and Galli, 2010;
75 Rotondi, 2012).

76



77

78

79 **Fig. 1.** (a) A view of the Villa dei Quintili (Rome, Italy). (b) Details of the archaeological site.

80

81 Built by the family of the Quintili brothers during the late Hadrian period (first half of the second
82 century A. D.), it underwent a series of construction phases until the Middle and Modern Ages. The
83 Villa assumes particular archaeological relevance in view of the high quality of the buildings and
84 decorative materials. Opus sectile and polychrome mosaics generally constitute the ornamental
85 elements of the floors, marbles, frescoes and mosaics those of the walls. Furthermore, in later times,
86 this residential complex became a centre of recycling and production of a variety of materials,
87 including glasses, marbles, frescoes and tuffs (Basso et al., 2014). This contributed to get complicated
88 the case study of this site, since the most part of these materials, and in particular frescoes fragments,
89 have been moved away from their original location and reused.

90 The six plasters under investigation in the present work are examples of this complex task. Taken
91 from the warehouse of the Villa, and hence of unknown provenance area, they have been already
92 subjected to an X-ray fluorescence (XRF) analysis in order to identify the elemental constituents of
93 the pigmenting agents (Alberti et al., 2017). Nevertheless, at that time, the investigation of the
94 molecular nature of pigments, necessary for their unambiguous identification, performed by means
95 of a portable Raman spectrometer, gave unreliable results because of the organic layers that covered
96 the samples, originating a high fluorescence that completely masked the signal coming from the
97 pigment. This is, unfortunately, the main disadvantage of portable equipments, that don't have
98 confocal attitude and micro-head.

99 Here, we have been able to overcome this difficulty by carrying out measurements using a micro-
100 Raman set-up working with different wavelengths of excitation, in the visible and middleUV range,
101 so increasing the signal-to-noise ratio and reducing the sample areas down to a few of μm^2 .

102 Data have been integrated by FT-IR spectroscopy measurements for the characterization, at
103 molecular level, of the painted surfaces (supporting Raman results) and the bulk, by optical
104 microscopy (OM) observation, in order to gather information on the textural characteristics of sample
105 layers, and Scanning Electron Microscopy/Energy Dispersive Using X-Ray (SEM-EDX) analysis for
106 studying the morphology and the chemical composition of the samples.

107

108 **2. Material and methods**

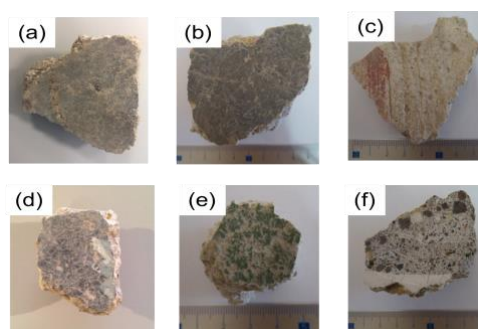
109

110 *2.1 Materials*

111

112 Measurements have been performed on six fresco fragments, dated back II century A. D., referred
113 as Cod. r19a, Cod. r19b, Cod. r19c, Cod. r19d, Cod. r19f, Cod. section. Their representative images
114 are shown in Fig. 2.

115



116

117

118 **Fig. 2.** Photographs of analysed fragments. (a) Fresco Cod. r19a, (b) Fresco Cod. r19b, (c) Fresco Cod. r19c, (d) Fresco
119 Cod. r19d, (e) Fresco Cod. r19f, (f) Fresco Cod. section.

120

121 As already said in the Introduction, samples are taken from the warehouse of Villa dei Quintili, as
122 a consequence their provenance is unknown. The sample selection was undertaken under the
123 supervision of the archaeologists from the Archaeological Superintendence of Rome, in order to select
124 representative fragments.

125 The macroscopic features of the investigated frescoes are reported in Table 1, together with an
126 indication of the previously (Alberti et al., 2017) and present performed analyses.

127

128 **Table 1**

129 Macroscopic features of investigated frescoes together with the employed analytical techniques.

130

Sample	Description	Employed techniques
--------	-------------	---------------------

Cod. r19a	Fragment of fresco with two pigmented areas: yellow and black	SEM-EDX, FT-IR, micro-Raman
Cod. r19b	Fragment of fresco with a green pigmented area	XRF (previously), SEM-EDX, FT-IR, micro-Raman
Cod. r19c	Fragment of fresco with two pigmented areas: red and white	XRF (previously), SEM-EDX, FT-IR, micro-Raman
Cod. r19d	Fragment of fresco with two pigmented areas: blue and white	XRF (previously), OM, SEM-EDX, FT-IR, microRa
Cod. r19f	Fragment of fresco with a green pigmented area	XRF (previously), OM, SEM-EDX, FT-IR, microRa
Cod. section	Fragment of fresco with three pigmented areas: brown, dark brown and white	man XRF (previously), SEM-EDX Mapping, FT-IR, micro-Raman

131

132 2.2 Methods

133

134 2.2.1 OM and SEM-EDX analyses

135

136 Some micro-samples, bearing the characteristic of the whole stratigraphy, were collected by a
137 scalpel from every fragment of fresco. Cross-sections were obtained by embedding the samples into
138 epoxy resin (Epofix Struers and Epofix Hardener with ratio 15:2) and by polishing them with silicon
139 carbide fine sandpaper (800-4000 mesh). The polished cross-sections were thus observed through a
140 polarized light optical microscope Olympus BX51TF equipped with an Olympus TH4200 lamp
141 (visible light) and an Olympus U-RFL-T (UV radiation). Imaging at higher magnifications and micro-
142 analyses were performed by SEM-EDX using a FE-SEM Tescan Mira 3XMU-series (Brno, Czech
143 Republic), set with an accelerating voltage of 15-20 kV in high vacuum and equipped with a Bruker
144 Quantax 200 Energy-Dispersive X-ray spectrometer. Before the SEMEDX investigation, the samples
145 were made conductive with a graphite coating obtained by a Cressington Carbon Coater 208C. Data
146 were then processed using the Bruker Esprit 2 microanalysis software.

147

148 2.2.2 Micro-Raman analyses

149

150 Micro-Raman spectra were obtained, in non invasive way, by means of a LabRam HR800 Raman
151 confocal Micro-Spectrometer (Horiba-Jobin Yvon) in the back-scattering configuration and making
152 use of excitation wavelengths ranging from the near UV to the near infrared. Indeed, this setup allows
153 for a multi-wavelength excitation being coupled to a He-Ne laser (633 nm), an argonion laser used to

154 produce the UV line at 364 nm, a solid state laser at 561 nm and a diode laser at 785 nm. The laser
155 beams at $\lambda_{exc} = 633$ nm, 561 nm and 785 nm were focused by means of a microscope objective 50X
156 Long Working Distance (Olympus LM-Plan-Fl, NA = 0.5, power of 0.5 mW on samples) mounted
157 on an Olympus BX41-microscope, while the UV line was used focused by means of a 60X fluorite
158 objective microscope (Olympus UPlan FLN, NA = 0.9, power of 0.5 mW on samples). During the
159 measurements the scattered radiation was dispersed by a 600 l/mm grating and collected by a silicon
160 CCD as detector (Synapse, Horiba-Jobin Yvon). For each sample we chose the excitation wavelength
161 which gave the best Raman response, in order to overcome problems arising from fluorescence
162 contribution to the spectrum. For each spectrum reported in the Results and Discussions section, the
163 chosen wavelength is indicated in the corresponding figure caption.

164 The obtained spectra were compared with those of various databases and literature (Bell et al.,
165 1977; Buzgar et al., 2009; RRUFF Project, 2010).

166

167 2.2.3 FT-IR analyses

168

169 FT-IR spectra were collected, in micro-invasive way, in the $400 \div 4000$ cm^{-1} wavenumber region
170 with a resolution of 4 cm^{-1} , using a Bomem DA8 Fourier transform spectrometer, operating with a
171 Global source, combined with a KBr beamsplitter, and a DTGS/MIR detector. The IR spectra were
172 recorded on the samples in the form of pellets, by taking ~ 2 mg of sample, that has been powdered
173 and dispersed in ~ 200 mg of a powdered CsI matrix, transparent in the investigated range. The
174 measurements were performed in transmission configuration and in dry atmosphere to avoid
175 unwanted dirty contributions, automatically adding 32 repetitive scans in order to guarantee good
176 signal-to-noise ratio and high spectral reproducibility.

177 No smoothing was applied, and Spectracalc software package GRAMS (Galactic Industries,
178 Salem, NH, USA) was used for baseline correction.

179 The identification of pigments and accessory components has been achieved by comparison of the
180 experimental profiles with those of various databases and literature (De Benedetto et al., 2002; Sadtler
181 Database for FT-IR, BioRad Laboratories).

182

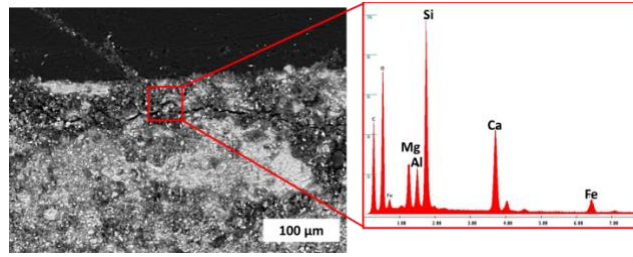
183 3. Results and Discussion

184 Generally, in most of the cross sections, the "intonachino" layer is absent below the pictorial film.
185 The pigmenting phase is therefore in direct contact with the underlying "curl" level. In the "arriccio"
186 layer are dispersed different deposits, with rounded and sub-rounded clasts and with a good

187 granulometric selection. In almost all the samples, except for r19c, the composition of the aggregate
188 is rich in female minerals (amphiboles and pyroxenes associated with quartz and feldspars). The
189 smaller sizes are absent, perhaps indicating a washing of the material before use and therefore
190 suggesting a good level of preparation. The sediment seems to be rich in volcanic material. An
191 estimate of the amount of aggregate averages between 40 and 60%.

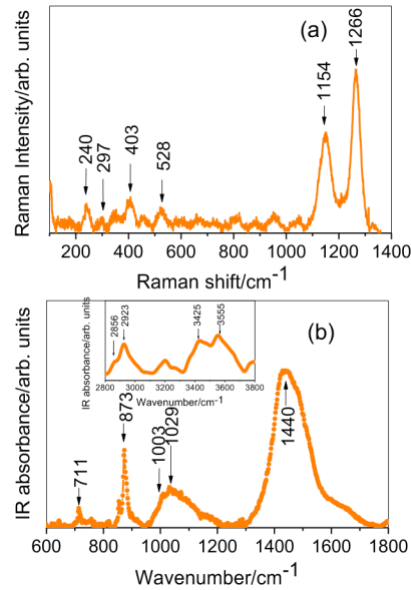
192 **Fresco Cod. r19a.** The SEM visual examination performed on the cross section of fresco
193 highlighted an homogeneous layer of pigments along the surface with a thickness of about 50 μm .
194 The EDX analysis carried out the pictorial layer revealed the presence of low signal of Fe, probably
195 ascribable to the yellow pigment, and stronger emission peaks of Ca, Si, Mg and Al, due probably to
196 the presence of feldspars (Fig. 3). Raman spectrum collected on the yellow pigment (Fig. 4(a)) clearly
197 evidenced the typical bands of goethite ($\alpha\text{-FeOOH}$) at $\sim 240\text{ cm}^{-1}$, $\sim 298\text{ cm}^{-1}$, $\sim 403\text{ cm}^{-1}$, $\sim 528\text{ cm}^{-1}$.
198 The identified pigment is then yellow ochre, whose use is largely documented in the case of Roman
199 wall paintings (Aliatis et al., 2010). In the $1100 \div 1400\text{ cm}^{-1}$ region characteristic features of a fatty
200 acid medium are well evident. The observed bands at $\sim 1154\text{ cm}^{-1}$ and $\sim 1266\text{ cm}^{-1}$ suggest, from
201 comparison with literature data (Schönemann et al., 2011; Vandenabeele et al., 2000), the use of
202 linseed oil. In the FT-IR spectrum (Fig. 4(b)), contributions attributed to calcite (CaCO_3 , peaks at \sim
203 711 cm^{-1} , $\sim 873\text{ cm}^{-1}$, band centred at $\sim 1440\text{ cm}^{-1}$), feldspars (broad band between $\sim 950\text{ cm}^{-1}$ and
204 $\sim 1270\text{ cm}^{-1}$) and gypsum ($\text{CaSO}_4 \cdot 2\text{H}_2\text{O}$, broad band between $\sim 950\text{ cm}^{-1}$ and $\sim 1270\text{ cm}^{-1}$ and band
205 centred at $\sim 1440\text{ cm}^{-1}$), have been recognized. In particular, the presence of the double peak at \sim
206 1003 cm^{-1} and $\sim 1029\text{ cm}^{-1}$ deserves attention. These lines correspond to Si-O-Al and SiO-Si
207 stretching vibrations and play an important role in identifying ochre components. Furthermore, as far
208 as the high frequency range of the FT-IR spectrum is concerned (inset of Fig. 4(b)), the peaks in the
209 $2800 \div 3000\text{ cm}^{-1}$ region are attributed to the C-H stretching mode of linseed oil, in agreement with
210 Raman results, whereas those in the $3300 \div 3800\text{ cm}^{-1}$ range, indicative of the O-H stretching
211 vibration, suggest that the feldspar present is kaolinite ($\text{Al}_2\text{Si}_2\text{O}_5(\text{OH})_4$). The result of goethite is
212 interesting because this kind of yellow ochre was used since the Paleolithic age, and researchers have
213 recognized goethite in pigments from ancient Egyptian specimens and have characterized it in Roman
214 wall paintings from England. Goethite in this case is the main constituent of the yellow ochre and this
215 result will be compared with the fresco still conserved *in situ*.

216



217
218
219
220

Fig. 3. (left) cross section of sample from r19a fresco, (right) EDX spectrum performed on the pictorial layer.



221
222

Fig. 4. (a) Raman spectrum recorded at $\lambda_{exc} = 785$ nm on yellow pigment of fresco Cod. r19a. (b) FT-IR spectrum recorded on yellow pigment of fresco Cod. r19a. In the inset, the high frequency range of the FT-IR spectrum is shown.

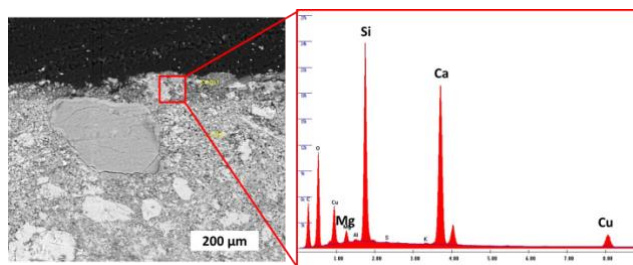
225

226 As far as the black pigment is concerned, FT-IR spectrum evidenced only the absorption peaks of
227 calcite. This allowed us to hypothesize the presence of carbon black (Bakiler et al., 2016; Mahmoud
228 et al., 2000), used as decorative pigment since the earliest times. The vegetal origin of the pigment is
229 also confirmed by Raman analysis, that detected no band at ~ 960 cm^{-1} , associated to the stretching
230 of the phosphate ion $[\text{PO}_4]^{3-}$, and revealed the characteristic two-band feature at ~ 1335 cm^{-1} and \sim
231 1565 cm^{-1} .

232 **Fresco Cod. r19b.** The SEM study of the cross section reveals a structure of the mortar ground
233 with grains different in size and crystal habit, that is typical of roman fresco grounds. In this case, the
234 painting layer shows a low thickness and a not homogeneous coat along the surface, maybe due to a
235 strong alteration process of the pigment. The presence of typical elements of feldspars (Ca, Si, Mg

236 and Al) has been detected by EDX analysis (Fig. 5), associated to a characteristic emission of Cu,
237 probably due to the use of a green earth as pigment.

238



239

240

1

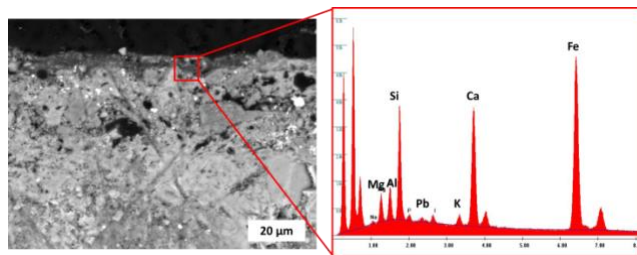
Fig. 5. (left) SEM image of cross section sample from r19b fresco, (right) EDX spectrum performed on the pictorial 2 layer.

3

4 Previous XRF analysis on the green pigment (Alberti et al., 2017) didn't provide enough
5 information for the identification of the pigment, probably because of a too low concentration of the
6 pigment itself or a too limited thickness of the paint layer. Raman analysis in this case, probably for
7 the aforementioned reasons, didn't furnish reliable results. Nevertheless, FT-IR spectra evidenced,
8 other than the characteristic peaks of the base, a peak at $\sim 798 \text{ cm}^{-1}$, that seems to confirm the use
9 of a green earth, in agreement with SEM-EDX results.

10 **Fresco Cod. r19c.** As the r19b sample, SEM-EDX analysis performed on the red layer of the
11 cross section (Fig. 6) highlight signals related to the presence of feldspars ascribable to the mortar
12 of the ground. A strong Fe signal has been detected in the same layer, probably due to the presence
13 of a red earth. It's interesting to highlight in the same layer the presence of a weak Pb signal: this
14 element seems to be related to the use of white lead just under the pictorial film or mixed with
15 pigment, maybe in order to obtain a brighter red color. The presence of lead in this cross section
16 could be used as a possible marker to recognize other frescos from the several fragments revealed
17 during the archeological site. Moreover, in this sample, a different structure of the ground mortar
18 is
19 detected, that appears in section more homogeneous than r19a and r19b samples without the grains
19 typical of the aggregate deposits.

20



21

22

23 **Fig. 6.** (left) SEM image of cross section sample from r19b fresco, (right) EDX spectrum performed on the pictorial 24 layer.

25

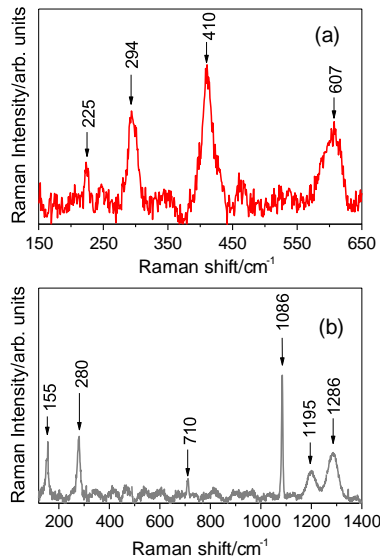
26 The Raman spectrum collected for the red pigment (Fig. 7(a)) confirmed the SEM-EDX results
27 and allowed, from the characteristic vibration modes at $\sim 225 \text{ cm}^{-1}$, $\sim 294 \text{ cm}^{-1}$, $\sim 410 \text{ cm}^{-1}$, and
~

28 607 cm^{-1} , for the identification of hematite ($\alpha\text{-Fe}_2\text{O}_3$), as usually found in red ochres. This result is
29 in agreement with previous XRF measurements (Alberti et al., 2017), that revealed the presence
of
30 iron as major element. Hematite belongs to the crystal space group of D_6^{3d} symmetry, that has
seven
31 Raman-active vibrational modes, i.e. two A_{1g} modes and five E_g modes (De Faria et al., 1997). In

1

1 particular, the strong band at $\sim 410 \text{ cm}^{-1}$ indicates that a well-crystallized hematite was used. The use
2 of a red ochre is also confirmed by looking at the FT-IR spectrum (red line of Fig. 8), that showed,
3 other than bands attributed to calcite ($\sim 715 \text{ cm}^{-1}$, $\sim 874 \text{ cm}^{-1}$, $\sim 1437 \text{ cm}^{-1}$), features centered at \sim
4 537 cm^{-1} and $\sim 910 \text{ cm}^{-1}$, assigned to iron oxides. In addition, in the large band between $\sim 940 \text{ cm}^{-1}$
5 and $\sim 1280 \text{ cm}^{-1}$, mainly associated to feldspars and gypsum, contributions of iron oxides at ~ 1011
6 cm^{-1} and $\sim 1050 \text{ cm}^{-1}$ also appear.

7



8

9

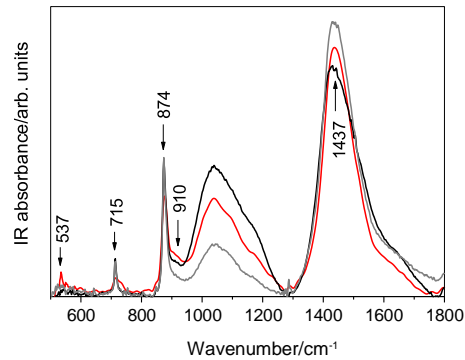
10 **Fig. 7.** (a) Raman spectrum recorded at $\lambda_{\text{exc}} = 785 \text{ nm}$ on red pigment of fresco Cod. r19c. (b) Raman spectrum recorded
11 at $\lambda_{\text{exc}} = 785 \text{ nm}$ on white pigment of fresco Cod. r19c.

12

13 White paint layer of fresco Cod. r19c contained lime white, based on the Raman bands (Fig. 7(b))
14 at $\sim 155 \text{ cm}^{-1}$, $\sim 280 \text{ cm}^{-1}$, $\sim 710 \text{ cm}^{-1}$, and $\sim 1086 \text{ cm}^{-1}$, corresponding to calcite. The well evident
15 profiles in the amide III region ($1100 \div 1400 \text{ cm}^{-1}$) reveal the use of a proteinaceous binder, probably
16 linseed oil, as suggested by comparison with literature data (Schönemann et al., 2011; Vandenaabeele
17 et al., 2000). FT-IR technique gave evidence of calcite, gypsum and feldspars (white line of Fig. 8).
18 It is worth of note that, comparing the FT-IR spectrum of white pigment with that of the bulk of the
19 same sample (black line of Fig. 8), contributions due to calcite appears much more intense with
20 respect to those due to gypsum and feldspars. This occurrence supports the hypothesis of the use of
21 lime white as white pigment, as evidenced by Raman spectroscopy. Nevertheless, this enhancement
22 can also be due to the preparatory layers of lime plaster. Finally, the use of the organic binder in the

23 white painted surface is also testified by the presence, in the high frequency region of the FT-IR
24 spectrum, not reported here, of several bands in the 2800 ÷ 3000 cm⁻¹ interval.

25



26

27

28

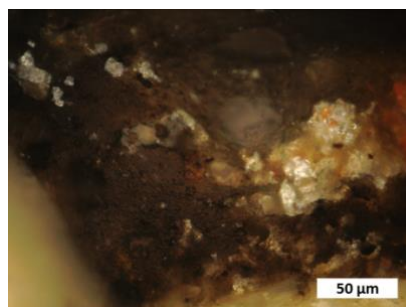
29 **Fig. 8.** FT-IR spectra recorded on the bulk (black line), red pigment (red line) and white pigment (white line) of fresco
30 Cod. r19c.

31

32 Traces of blue pigment were also present on the painted surface of the fresco. Nevertheless,
33 unfortunately, the micro-Raman spectrum, collected using an excitation wavelength of 785 nm, was
34 completely covered by a very strong fluorescence. Also FT-IR measurements, because of the too
35 small amount of sample, resulted unreliable.

36 **Fresco Cod. r19d.** The study of the cross section under optical microscopy (Fig. 9) shows a
37 painted layer with a brown binder and different grains in colour and shapes. The blue particles appear,
38 under OM, grey and shiny, mixed with orange and white grains. The SEM-EDX analysis performed
39 on this area (Fig. 10) highlights some intense emission peaks related to the presence of Si, Ca and Cu,
40 with some weak peak due to Mg, Al, K and S. The presence of Cu suggests the presence of a copper
41 based mineral used as blue pigment. The presence of Si and Ca could be ascribed to quartz and
42 calcium carbonate (CaCO₃). Finally, the observation of Mg, Al and K together with Ca and Si allows
43 to hypothesize the presence of aluminium silicates (feldspar). Even in this case the mortar shows the
44 same aggregate compositions in grains with different size and shape.

45



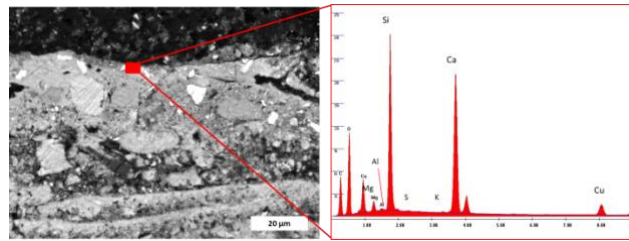
46

1

47

48 **Fig. 9.** OM image of the painting film with magnification of grains.

49



50

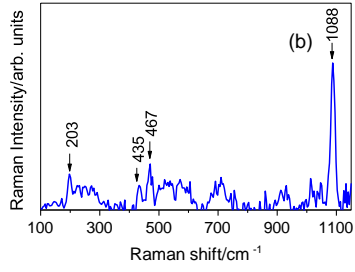
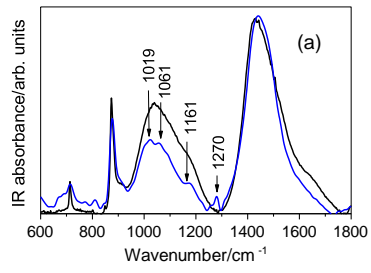
51

52 **Fig. 10.** (left) SEM image of cross section sample from r19d fresco, (right) EDX spectrum performed on the pictorial
53 layer.

54

55 Raman spectrum of the blue painted layer of this sample was first of all collected by using an
56 excitation wavelength of 785 nm, and no bands were recorded. Nevertheless, SEM-EDX analysis
57 allowed us to hypothesize that the used blue pigment consisted mainly of copper, and FT-IR analysis
58 (Fig. 11(a)) indicates the presence of cuprorivaite ($\text{CaCuSi}_4\text{O}_{10}$), whose characteristic features are
59 centred at $\sim 1019 \text{ cm}^{-1}$, $\sim 1061 \text{ cm}^{-1}$, $\sim 1161 \text{ cm}^{-1}$ and $\sim 1270 \text{ cm}^{-1}$. Now, since it has been reported
60 (Westlake et al., 2012) that Egyptian blue, when excited in the visible and NIR range, exhibits strong
61 fluorescence emission with a maximum at $\sim 890 \text{ nm}$, the use of a laser line in the UV range (364 nm)
62 became mandatory. The recorded spectrum is reported in Fig. 11(b). By the typical peaks at ~ 435
63 cm^{-1} and $\sim 1088 \text{ cm}^{-1}$, the blue pigment was identified as Egyptian blue, in agreement with a variety
64 of studies on wall paintings of Roman period (Aliatis et al., 2010; Mahmoud et al., 2000; Mateos et
65 al., 2015; Mazzocchin et al., 2010). Quartz (SiO_2) is also detected by the observation of the typical
66 features at $\sim 203 \text{ cm}^{-1}$ and $\sim 467 \text{ cm}^{-1}$.

67



1

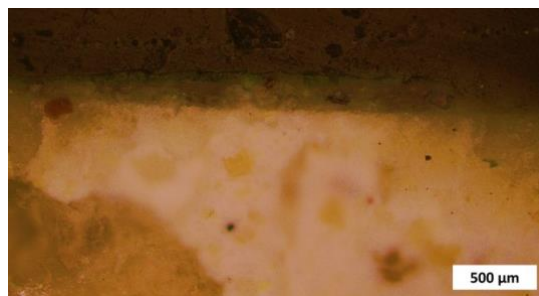
2 **Fig. 11.** (a) FT-IR spectrum recorded on blue pigment (blue line) of fresco Cod. r19d. The FT-IR spectrum recorded on 3 the
bulk (black line) of the same sample is reported for comparison. (b) Raman spectrum recorded at $\lambda_{exc} = 364$ nm on 4 blue
pigment of fresco Cod. r19d.

5

6 As far as the white pigment is concerned, Raman and FT-IR measurements (spectra not reported)
7 gave evidence of calcite, gypsum and feldspars, probably also due to the preparation layer and
8 plaster. In the FT-IR spectrum, in particular, characteristic contributions of Egyptian blue were
9 recognized, in agreement with previous XRF results (Alberti et al., 2017) that revealed, other than
10 Ca, also the presence of Cu in some amount. This occurrence can indicate that the artist wanted a 11
different shade for this specific part of the decoration.

12 **Fresco Cod. r19f.** The cross section studied under optical microscopy (Fig. 12) shows a clear
13 homogeneous green layer well preserved applied directly on a typical roman lime ground, with
14 grains of different diameter and shapes. Even in this case, the "intonachino" layer is absent below
15 the pictorial film and the pigmentation phase is in direct contact with the underlying "curl" level, 16
confirming this procedure as a construction marker of the frescos of the Villa.

17



18

19

20 **Fig. 12.** OM image of the r19f cross section with green pictorial film.

21

22 The SEM-EDX analysis (Fig. 13) performed on the coloured layer highlighted an intense peak
23 related to Fe, probably ascribable to the presence of an earth pigment, and the absence of the Cu
24 peak, as expected. The presence of Si, Mg, Al and K emissions could be ascribable to the earth
too,

25 and this seems to be confirmed by the presence of a weak peak of Ti. Ca is present in the spectrum
26 with a strong peak probably due to the inorganic binder of the fresco (CaCO_3).

27

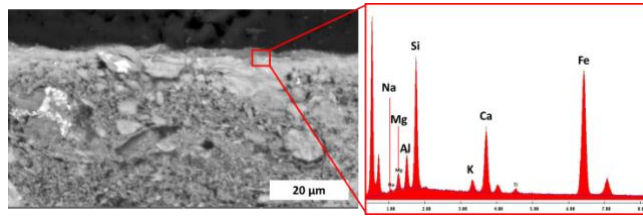


Fig. 13. (left) SEM image of cross section sample from r19f fresco, (right) EDX spectrum performed on the pictorial layer.

Raman spectrum of the green painted layer (Fig. 14) clearly shows typical peaks of calcite (~ 152 cm^{-1} and ~ 1086 cm^{-1}), probably due to lime present in the wall preparatory layer, and green earth of celadonite ($\text{K}(\text{Mg}, \text{Fe}^{2+})(\text{Fe}^{3+}, \text{Al})[\text{Si}_4\text{O}_{10}](\text{OH})_2$) nature (~ 203 cm^{-1}), commonly identified in Roman wall paintings from different localities (Aliatis et al., 2009; Béarat and Fuchs, 1996; Mazzocchin et al., 2003; Villar and Edwards, 2005).

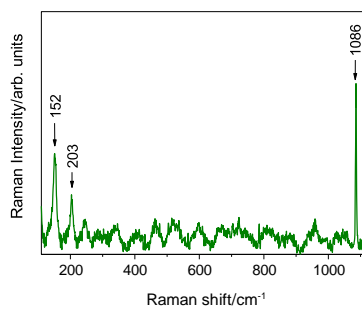
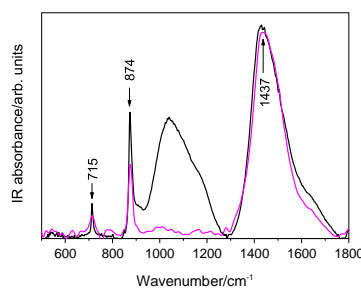


Fig. 14. Raman spectrum recorded at $\lambda_{\text{exc}} = 785$ nm on green pigment of fresco Cod. r19f.

In order to gain information on the composition of the plaster layers, FT-IR and Raman measurements have been also performed on a point at the base without any pigment and on the bulk of this sample. The comparison of the FT-IR spectra obtained in these two cases, reported in Fig. 15, looks particularly interesting.



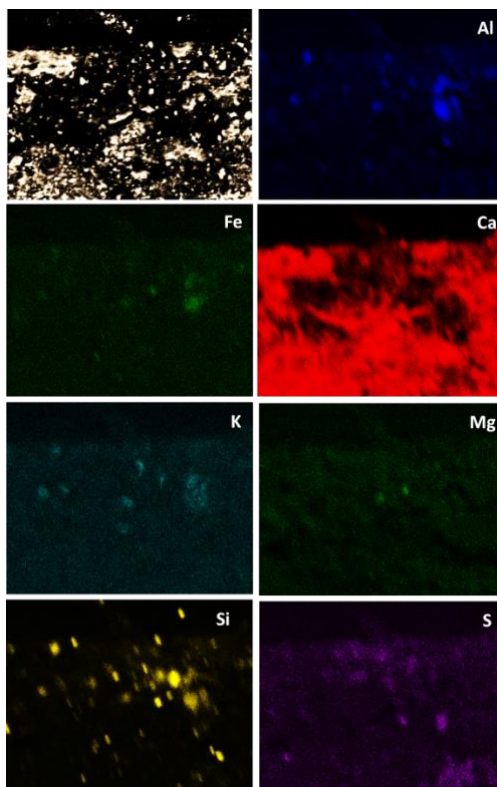
25 **Fig. 15.** FT-IR spectrum recorded on a point at the base without any pigment (magenta line) and on the bulk (black line)
26 of fresco Cod. r19f.

27

28 The two spectra appears similar, both of them contain the main characteristic peaks of calcite.
29 Nevertheless, these are the only contributions in the case of the point at the base without any pigment
30 (magenta line of Fig. 15). This was confirmed also by Raman technique that evidenced, for the point
31 at the base without any pigment, only peaks attributable to calcite (spectrum not reported). On the
32 contrary, in the FT-IR spectrum of the bulk (black line of Fig. 15), the large band between $\sim 940\text{ cm}^{-1}$
33 1 and $\sim 1280\text{ cm}^{-1}$ due to feldspars and gypsum is also well evident. We can then argue that the fine
34 plaster “intonaco” is mainly based on calcite. As Vitruvius reported in his work *De Architectura* (I
35 century B. C.) (Vitruvius, 1914), limewash was very commonly used in Roman walls before painting,
36 and the result of this practice was calcium carbonate obtained by reaction of lime (calcium hydroxide)
37 with atmospheric carbon dioxide. As far as the second layer “arriccio” is concerned, it is mainly
38 composed by calcite, feldspars and gypsum.

39 **Fresco Cod. section.** Due to the not homogeneous painted layer of the fresco and in order to better
40 consider the distribution of the different elements and, consequently, of the mineral grains, a SEM-
41 EDX mapping analysis has been performed on the cross section of this sample. As can be seen from
42 an inspection of Fig. 16, Ca is well dispersed out among the section, confirming the presence of
43 CaCO_3 as the inorganic binder of the fresco. Al, Si, K and Fe are concentrated in the same area of the
44 cross section and therefore ascribable to the same mineral phase, probably an earth. The S element,
45 that could be ascribed to gypsum, seems to be distributed in the area where Ca is not present. This
46 result seems to confirm the degradation process of chemical transformation from carbonate to
47 sulphate.

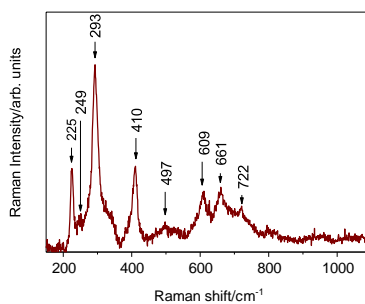
48



49
50
51
52
53
54
55
56
57

Fig. 16. SEM-EDX mapping of Cod. section.

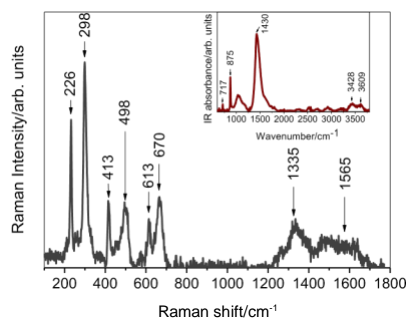
The Raman spectrum collected on the brown pigment is reported in Fig. 17. All peaks relative to haematite, centered at $\sim 225 \text{ cm}^{-1}$, $\sim 249 \text{ cm}^{-1}$, $\sim 293 \text{ cm}^{-1}$, $\sim 410 \text{ cm}^{-1}$, $\sim 609 \text{ cm}^{-1}$, $\sim 661 \text{ cm}^{-1}$, have been identified. In addition, the features at $\sim 497 \text{ cm}^{-1}$ and $\sim 722 \text{ cm}^{-1}$ are associated to maghemite ($\text{g-Fe}_2\text{O}_3$).



58
59
60
61
62
63
64

Fig. 17. Raman spectrum recorded at $\lambda_{\text{exc}} = 785 \text{ nm}$ on brown pigment of fresco Cod. section.

Fig. 18 shows the Raman spectrum for the dark brown pigmented area of the sample.



65
66

67

68 **Fig. 18.** Raman spectrum recorded at $\lambda_{exc} = 633$ nm on dark brown pigmented area of fresco Cod. section. In the inset, FT-
69 IR spectrum of the same specimen is depicted.

70

71 The spectrum contains a series of bands in the region between 200 cm^{-1} and 800 cm^{-1} , that are all
72 those identified in the Raman spectrum of red ochre, which consists of a mixture of silica, clay and
73 iron oxide (Bikiaris et al., 1999). In particular, the Raman peak at $\sim 670\text{ cm}^{-1}$ is attributed to Al-OSi
74 bond of kaolinite (Frost et al., 1993). Kaolinite has a weak white colour, that lends luminance to red
75 ochre.

76 The two bands at $\sim 1335\text{ cm}^{-1}$ and $\sim 1565\text{ cm}^{-1}$ reveals the presence of carbon, probably used to
77 darken the red colour.

78 It is worth remarking that the obtained results are, once again, supported by previous XRF analysis
79 (Alberti et al., 2017). From that, Fe, K and Sr were identified for brown and dark brown points,
80 suggesting the presence of clays in their composition, also present in the materials used for the
81 preparation of the base. As a matter of fact, IR spectra collected on these two pigments (the case of
82 dark brown pigmented area is plotted in the inset of Fig. 18) evidenced the presence of clayey
83 minerals, such as calcite (peaks at $\sim 717\text{ cm}^{-1}$, $\sim 875\text{ cm}^{-1}$, $\sim 1430\text{ cm}^{-1}$), kaolinite and
84 montmorillonite (peaks in the $3300 \div 3800\text{ cm}^{-1}$ range).

85 Finally, as far as the white pigmented area is concerned, characteristic peaks of calcite are clearly
86 evident in the Raman spectrum, indicating calcite as the compound responsible for the white pigment.
87 IR profile showed bands attributed to calcite, gypsum, silicates and feldspars (spectra not reported).

88

89 4. Conclusions

90

91 In the present paper, we used a combined methodological approach, performed through optical
92 microscopy (OM), scanning electron microscopy equipped with an energy dispersive X-ray detector
93 (SEM-EDX), micro-Raman and Fourier transform infrared spectroscopy (FT-IR) techniques, in order

94 to identify the palette of pigments found in Roman wall paintings from the archaeological context of
95 Villa dei Quintili (Rome, Italy), dated back II century A. D..

96 From the results, the yellow pigment was identified as yellow ochre, the black pigment as carbon
97 black of vegetal origin, the red pigment as red ochre (haematite), the white pigment as lime white and
98 maybe lead white pigment, the blue pigment as Egyptian blue, the green pigment as green earth of
99 celadonite nature and, finally, the brown pigment as red ochre (haematite and maghemite) brightened
100 by kaolinite.

101 The fine plaster “intonaco” turned out to be mainly based on calcite, whereas calcite, feldspars and
102 gypsum resulted the main constituents of the second layer “arriccio”.

103 Linseed oil and calcium carbonate have been respectively recognized as organic and inorganic
104 binders, even if it’s not possible to exclude an application of those materials as protectives of the
105 fresco surfaces. Some compositional marker to classify the frescos on the basis of their properties and
106 to find a qualitative correlation with other fresco fragments extracted from other areas of the Villa,
107 have been characterized.

108

109 **Acknowledgments**

110

111 The authors acknowledge Dr. Rita Paris, Archaeologist Director of the Soprintendenza Speciale
112 per I Beni Archeologici di Roma, for supplying the investigated fragments of painted plasters,
113 withdrawn from the archaeological site of Villa dei Quintili (Rome, Italy).

114

115 **References**

116

117 Alberti, R., Crupi, V., Frontoni, R., Galli, G., La Russa, M. F., Licchelli, M., Majolino, D., Malagodi,
118 M., Rossi, B., Ruffolo, S. A., Venuti, V., 2017. Handheld XRF and Raman equipment for the in
119 situ investigation of Roman finds in the Villa dei Quintili (Rome, Italy). *J. Anal. At. Spectrom.* 32,
120 117-129.

121 Aliatis, I., Bersani, D., Campani, E., Casoli, A., Lottici, P. P., Mantovan, S., Marino, I. G., Ospitali,
122 F., 2009. Green pigments of the Pompeian artists' palette. *Spectrochim. Acta A* 73, 532-538.

123 Aliatis, I., Bersani, D., Campani, E., Casoli, A., Lottici, P. P., Mantovan, S., Marino, I. G., 2010.
124 Pigments used in Roman wall paintings in the Vesuvian area. *J. Raman Spectrosc.* 41, 15371542.

125 Amadori, M. L., Barcelli, S., Poldi, G., Ferrucci, F., Andreotti, A., Baraldi, P., Colombini, M. P.,
126 2015. Invasive and noninvasive analyzes for knowledge and conservation of Roman wall paintings
127 of the Villa of the Papyri in Herculaneum. *Microchem. J.* 118, 183-192.

- 128 Bakiler, M., Kırmızı, B., Öztürk, Ö. O., Hanyalı, Ö. B., Dağ, E., Çağlar, E., Köroğlu, G., 2016.
129 Material characterization of the Late Roman wall painting samples from Sinop Balatlar Church
130 Complex in the black sea region of Turkey. *Microchem. J.* 126, 263-273.
- 131 Baraldi, P., Baraldi, C., Curina, R., Tassi, L., Zannini, P., 2007. A Micro-Raman archaeometric
132 approach to Roman wall paintings. *Vibr. Spectrosc.* 43, 420-426.
- 133 Barilaro, D., Crupi, V., Interdonato, S., Majolino, D., Venuti, V., Barone, G., La Russa, M. F.,
134 Bardelli, F., 2008. Characterization of blue decorated Renaissance pottery fragments from
135 Caltagirone (Sicily, Italy). *Appl. Phys. A* 92, 91-96.
- 136 Basso, E., Invernizzi, C., Malagodi, M., La Russa, M. F., Bersani, D., Lottici, P. P., 2014.
137 Characterization of colorants and opacifiers in Roman glass mosaic tesserae through spectroscopic
138 and spectrometric techniques. *J. Raman Spectrosc.* 45, 238-245.
- 139 Béarat, H., Fuchs, M., 1996. Analyses physico-chimiques et minéralogiques de peintures murales
140 romaines d'Aventicum. I. Du pigment à Avenches. *Bull. Assoc. Pro Aventico* 38, 35-51.
- 141 Belfiore, C. M., Fichera, G. V., La Russa, M. F., Pezzino, A., Ruffolo, S. A., Galli, G., Barca, D.,
142 2015. A multidisciplinary approach for the archaeometric study of pozzolanic aggregate in Roman
143 mortars: the case of Villa dei Quintili (Rome, Italy). *Archaeometry* 57, 269-296.
- 144 Bell, I. M., Clark, R. J. H., Gibbs, P. J., 1977. Raman Spectroscopic Library of Natural and Synthetic
145 Pigments. <http://www.chem.ucl.ac.uk/resources/raman/>.
- 146 Bikiaris, D., Daniilia, S., Sotiropoulou, S., Katsimbiri, O., Pavlidou, E., Moutsatsou, A. P.,
147 Chryssoulakis, Y., 1999. Ochre-differentiation through micro-Raman and micro-FTIR
148 spectroscopies: application on wall paintings at Meteora and Mount Athos, Greece. *Spectrochim.*
149 *Acta A* 56, 3-18.
- 150 Buzgar, N., Apopei, A. I., Buzatu, A., 2009. Romanian Database of Raman Spectroscopy.
151 <http://rdrs.uaic.ro>.
- 152 Crupi, V., Galli, G., La Russa, M. F., Longo, F., Maisano, G., Majolino, D., Malagodi, M., Pezzino,
153 A., Ricca, M., Rossi, B., Ruffolo, S. A., Venuti, V., 2015. Multi-technique investigation of Roman
154 decorated plasters from Villa dei Quintili (Rome, Italy). *Appl. Surf. Sci.* 349, 924-930.
- 155 Crupi, V., Allodi, V., Bottari, C., D'Amico, F., Galli, G., Gessini, A., La Russa, M. F., Longo, F.,
156 Majolino, D., Mariotto, G., Masciovecchio, C., Pezzino, A., Rossi, B., Ruffolo, S. A., Venuti, V.,
157 2016. Spectroscopic investigation of Roman decorated plasters by combining FT-IR, microRaman
158 and UV-Raman analyses. *Vibr. Spectrosc.* 83, 78-84.
- 159 De Benedetto, G. E., Laviano, R., Sabbatini, L., Zambonin, P. G., 2002. Infrared spectroscopy in the
160 mineralogical characterization of ancient pottery. *J. Cult. Herit.* 3, 177-186.

161 De Faria, D. L. A., Silva, S. V., De Oliveira, M. T., Raman microspectroscopy of some iron oxides
162 and oxyhydroxides. *J. Raman Spectrosc.* 28, 873-878.

163 Duran, A., Perez-Rodriguez, J. L., Jimenez de Haro, M. C., Franquelo, M. L., Robador, M. D.,
164 2011. Analytical study of Roman and Arabic wall paintings in the Patio de Banderas of Reales
165 Alcazares' Palace using nondestructive XRD/XRF and complementary techniques. *J. Archaeol.*
166 *Sci.* 38, 2366-2377.

167 Edwards, H. G. M., Middleton, P. S., Jorge Villar, S. E., De Faria, D. L. A., 2003. Romano-British
168 wall-paintings II: Raman spectroscopic analysis of two villa sites at Nether Heyford, Northants.
169 *Anal. Chim. Acta* 484, 211-221.

170 Frontoni, R., 2000. *Forma Urbis-Itinerari nascosti di Roma Antica, ANNO V(7/8)*, Roma.

171 Frontoni, R., Galli, G., 2010. Calce e calcara nella Villa dei Quintili. *Arkos, Scienza e Restauro* 25,
172 66-73.

173 Frost, R. L., Fredericks, P. M., Bartlett, J. R., 1993. Fourier transform Raman spectra of kandite clays.
174 *Spectrochim. Acta A* 49, 667-674.

175 Mahmoud, H. M., 2000. Investigations by Raman microscopy, ESEM and FTIR-ATR of wall
176 paintings from Qasr el-Ghuieta temple, Kharga Oasis, Egypt. *Heritage Science* 2, 18.

177 Mahmoud, H. M., Kantiranis, N., Stratis, J., 2012. A technical characterization of roman plasters,
178 Luxor temple, Upper Egypt. *Mediterranean Archaeology and Archaeometry* 12, 81-93.

179 Mateos, L. D., Cosano, D., Mora, M., Muñiz, I., Carmona, R., Jiménez-Sanchidrián, C., Ruiz, J. R.,
180 2015. Raman microspectroscopic analysis of decorative pigments from the Roman villa of El
181 Ruedo (Almedinilla, Spain). *Spectrochim. Acta, Part. A* 151, 16-21.

182 Mazzocchin, G. A., Agnoli, F., Salvadori, M., Colpo, I., 2003. Analysis of pigments from Roman
183 wall paintings found in Vicenza. *Talanta* 61, 565-572.

184 Mazzocchin, G. A., Vianello, A., Minghelli, S., Rudello, D., 2010. Analysis of roman wall paintings
185 from the Thermae of "Iulia Concordia". *Archaeometry* 52, 644-655.

186 Rotondi, A., 2012. *Forma Urbis-Itinerari nascosti di Roma Antica, ANNO XVII(2)*, Roma.

187 RRUFF Project, 2010. Department of Geosciences, University of Arizona, Tucson, USA.
188 <http://rruff.info/>.

189 Schönemann, A., Edwards, H. G. M., 2011. Raman and FTIR microspectroscopic study of the
190 alteration of chinese tung oil and related drying oils during ageing. *Anal. Bioanal. Chem.* 400,
191 1173-1180.

192 Vandenberghe, P., Wehling, B., Moens, L., Edwards, H., De Reu, M., Van Hooydonk, G., 2000.
193 Analysis with micro-Raman spectroscopy of natural organic binding media and varnishes used in
194 art. *Anal. Chim. Acta* 407, 261-274.

- 195 Villar, S. E. J., Edwards, H. G. M., 2005. An extensive colour palette in Roman villas in Burgos,
196 Northern Spain: a Raman spectroscopic analysis. *Anal. Bioanal. Chem.* 382, 283-289.
- 197 Vitruvius, 1914. *The Ten Books on Architecture*, translated by M. H. Morgan, Oxford University
198 Press, London, 1914.
- 199 Weber, J., Prochaska, W., Zimmermann, N., 2009. Microscopic techniques to study Roman renders
200 and mural paintings from various sites. *Mater. Charact.* 60, 586-593.
- 201 Westlake, P., Siozos, P., Philippidis, A., Apostolaki, C., Derham, B., Terlix, A., Perdikatsis, V.,
202 Jones, R. E., Anglos, D., 2012. Studying pigments on painted plaster in Minoan, Roman and early
203 Byzantine Crete. A multi-analytical technique approach. *Anal. Bioanal. Chem.* 402, 14131432.
- 204

205 **Figure captions**

206

207 **Fig. 1.** (a) A view of the Villa dei Quintili (Rome, Italy). (b) Details of the archaeological site.

208

209 **Fig. 2.** Photographs of analysed fragments. (a) Fresco Cod. r19a, (b) Fresco Cod. r19b, (c) Fresco
210 Cod. r19c, (d) Fresco Cod. r19d, (e) Fresco Cod. r19f, (f) Fresco Cod. section.

211

212 **Fig. 3.** (left) cross section of sample from r19a fresco, (right) EDX spectrum performed on the
213 pictorial layer.

214

215 **Fig. 4.** (a) Raman spectrum recorded at $\lambda_{exc} = 785$ nm on yellow pigment of fresco Cod. r19a. (b)
216 FT-IR spectrum recorded on yellow pigment of fresco Cod. r19a. In the inset, the high frequency
217 range of the FT-IR spectrum is shown.

218

219 **Fig. 5.** (left) SEM image of cross section sample from r19b fresco, (right) EDX spectrum
220 performed on the pictorial layer.

221

222 **Fig. 6.** (left) SEM image of cross section sample from r19b fresco, (right) EDX spectrum
223 performed on the pictorial layer.

224

225 **Fig. 7.** (a) Raman spectrum recorded at $\lambda_{exc} = 785$ nm on red pigment of fresco Cod. r19c. (b)
226 Raman spectrum recorded at $\lambda_{exc} = 785$ nm on white pigment of fresco Cod. r19c.

227

228 **Fig. 8.** FT-IR spectra recorded on the bulk (black line), red pigment (red line) and white pigment
229 (white line) of fresco Cod. r19c.

230

231 **Fig. 9.** OM image of the painting film with magnification of grains.

232

233 **Fig. 10.** (left) SEM image of cross section sample from r19d fresco, (right) EDX spectrum
234 performed on the pictorial layer.

235

236 **Fig. 11.** (a) FT-IR spectrum recorded on blue pigment (blue line) of fresco Cod. r19d. The FTIR
237 spectrum recorded on the bulk (black line) of the same sample is reported for comparison. (b)
238 Raman spectrum recorded at $\lambda_{exc} = 364$ nm on blue pigment of fresco Cod. r19d.

239
240 **Fig. 12.** OM image of the r19f cross section with green pictorial film.

241
242 **Fig. 13.** (left) SEM image of cross section sample from r19f fresco, (right) EDX spectrum
243 performed on the pictorial layer.

244
245 **Fig. 14.** Raman spectrum recorded at $\lambda_{exc} = 785$ nm on green pigment of fresco Cod. r19f.

246
247 **Fig. 15.** FT-IR spectrum recorded on a point at the base without any pigment (magenta line) and
248 on the bulk (black line) of fresco Cod. r19f.

249
250 **Fig. 16.** SEM-EDX mapping of Cod. section.

251
252 **Fig. 17.** Raman spectrum recorded at $\lambda_{exc} = 785$ nm on brown pigment of fresco Cod. section.

253
254 **Fig. 18.** Raman spectrum recorded at $\lambda_{exc} = 633$ nm on dark brown pigmented area of fresco Cod.
255 section. In the inset, FT-IR spectrum of the same specimen is depicted.

256
257 **Table 1** Macroscopic features of investigated frescoes together with the employed analytical
258 techniques.